pH-Responsive Polyzwitterions: A Comparative Study of Acrylamide-Based Polyampholyte Terpolymers and Polybetaine Copolymers

Michael J. Fevola,* J. Kasey Bridges, Matthew G. Kellum, Roger D. Hester, Charles L. McCormick

Department of Polymer Science, University of Southern Mississippi, Box 10076, Hattiesburg, Mississippi 39406-0076

ABSTRACT: A comparative study of pH-responsive polyzwitterions (PZs) with polyampholyte or polybetaine architectures was conducted with well-defined model polymer systems. Low-charge-density PZs, including ampholytic terpolymers composed of acrylamide (AM), sodium 3-acrylamido-3-methylbutanoate, and (3-acrylamidopropyl-)trimethylammonium chloride and carboxybetaine copolymers composed of AM and 3-(3-acrylamidopropyldimethylammonio)propionate, were prepared via free-radical polymerization in $0.5M$ NaCl to yield ter- and copolymers with random termonomer and comonomer distributions. Sodium formate was used as a chain-transfer agent during the polymerizations to eliminate the effects of the monomer feed composition on the degree of polymerization (DP) and to suppress gel effects and broadening of the molecular weight distributions. The polymer compositions were determined via ^{13}C-NMR spectroscopy, and the residual counterion content was determined via elemental analysis for Na^+ and Cl^-. The molecular weights (MWs) and polydispersity indices (PDIs) were determined via size exclusion chromatography/multi-angle laser light scattering (SEC–MALLS); the polymer MWs ranged from 1.4 to 1.5×10^6 g/mol, corresponding to DPs of $1.6–1.9 \times 10^4$ repeat units, with all the polymers exhibiting PDIs less than or equal to 2.1. The intrinsic viscosities determined from SEC–MALLS data and the Flory–Fox relationship agreed with the intrinsic viscosities determined via low-shear dilute-solution viscometry. Data from the SEC–MALLS analysis were used to analyze the radius of gyration/molecular weight (R_g–M) relationships and the Mark–Houwink–Sakurada intrinsic viscosity/molecular weight ([η]–M) relationships for the PZs. The R_g–M and [η]–M relationships and viscometric data revealed that under size exclusion chromatography conditions, the poly[acrylamide-*co*-3-(3-acrylamidopropyldimethylammonio)propionate] betaine copolymers had more open, random-coil conformations and greater polymer–solvent interactions than the ampholytic poly[acrylamide-*co*-sodium 3-acrylamido-3-methylbutanoate-*co*-(3-acrylamidopropyl)-trimethylammonium chloride] terpolymers. The pH- and salt-responsive dilute-solution viscosity behavior of the PZs was examined to assess the effects of the polymer structure and composition on the solution properties. The polyampholyte terpolymers had greater solution viscosities and more pronounced stimuli-responsiveness than the polybetaine copolymers because of their stronger intramolecular interactions and increased chain stiffness. © 2004 Wiley Periodicals, Inc. J Appl Polym Sci 94: 24–39, 2004

Key words: monomers; water-soluble polymers

INTRODUCTION

Zwitterionic water-soluble polymers have been the subject of extensive investigations in our laboratories because of their unique responsiveness to saline media.[1,2] Unlike polyelectrolytes (PEs), which bear *either* anionic or cationic charges, polyzwitterions (PZs) bear *both* anionic and cationic functionalities.[3–5] PZs are categorized as polyampholytes (anionic and cationic charges on *separate* repeat units) or polybetaines (anionic and cationic charges on *the same* repeat unit).[1,6] Because of their zwitterionic character, PZs exhibit markedly different behavior than PEs in aqueous solutions.[4,6–12] In dilute, salt-free aqueous solutions, PEs adopt extended conformations and possess large hydrodynamic volumes because of the electrostatic repulsions of the like charges along the polymer chain;[13] as a result, PE solutions in fresh water tend to maintain high viscosities. However, PEs usually exhibit decreases in the hydrodynamic volume and solution viscosity upon the addition of electrolytes with low molecular weights (MWs; e.g., salts). This PE effect is due to conformational changes that occur when the added electrolytes shield the electrostatic repulsions of like charges along the polymer chain, causing the polymer coils to contract. On the other hand, PZs tend

to adopt collapsed or globular conformations in salt-free solutions because of the electrostatic attractions between opposite charges.[9,11] Indeed, the electrostatic associations are so strong in PZ solutions that the polymers may phase-separate in the absence of low-MW electrolytes. However, as simple electrolytes are added to PZ solutions, the electrostatic interactions are shielded, and the PZs can adopt random-coil conformations. Sometimes called the *antipolyelectrolyte effect*, the globule-to-coil transition that occurs upon the addition of electrolytes results in increased polymer hydrodynamic volume and solution viscosity.

Many factors govern PZ solution properties, including the charge density, charge asymmetry (i.e., degree of charge imbalance), and chemical properties of the ionizable groups.[1,4,5,9,11,12,14] The PZ solubility and magnitude of the globule-to-coil transition (i.e., change in the hydrodynamic size) exhibited by PZs are typically determined by the charge density of the system. As the PZ charge density increases, greater concentrations of electrolytes are required to elicit coil expansion, and the relative increase in the hydrodynamic size upon electrolyte addition tends to be greater. Unbalanced PZs (i.e., PZs with a net charge) usually exhibit a combination of PZ and PE solution behavior according to the degree of charge imbalance. PZs generally tend to exhibit behavior more characteristic of conventional PEs with increasing charge asymmetry. For PZs bearing weakly acidic and/or weakly basic functional groups (i.e., carboxylic acids and/or tertiary amines), the charge density and charge asymmetry are dictated by the level of functional group incorporation and the solution pH; therefore, reversible transitions between PE and PZ behavior can be triggered by changes in the solution pH.

Synthetic PZs based on polyacrylamide (PAM) have been the focus of extensive study in academic and industrial laboratories because of their potential for application in petroleum production, drag reduction, suberabsorbants, water treatment, and the formulation of pharmaceuticals, cosmetics, and personal care items.[15–37] PAM-based polyampholytes are obtained via the terpolymerization of acrylamide (AM) with cationic and anionic comonomers, whereas PAM-based polybetaines are prepared via the copolymerization of AM with zwitterionic or inner salt monomers. Low-charge-density PZs incorporating high levels of AM are particularly desirable, as long runs of hydrophilic AM repeat units increase polymer solubility at low solution ionic strengths; therefore, less added electrolyte is required for dissolution. Low-charge-density PZs typically exhibit greater viscosifying ability than high-charge-density PZs, and the incorporation of relatively inexpensive nonionic monomers (e.g., AM, *N,N*-dimethylacrylamide, and *N*-vinylpyrrolidone) allows for the synthesis of more cost-efficient PZ systems with enhanced performance.

Most PAM-based PZs reported in the literature contain ionic functional groups that are not sensitive to changes in the solution pH. For example, most PAM-based polyampholyte terpolymers are composed of AM, a sulfonated anionic monomer [e.g., sodium 2-acrylamido-2-methylpropanesulfonate (NaAMPS) or sodium styrenesulfonate], and a quaternary ammonium cationic monomer [e.g., (3-methacrylamidopropyl)trimethylammonium chloride, (2-methacryloyloxyethyl)-trimethylammonium chloride, or (2-acrylamido-2-methylpropyl)trimethylammonium chloride (AMPTAC)].[3,17,21,25,30] Because of the non-pH-responsive nature of these monomers, the charge balance of these systems is determined solely by the relative incorporation of cationic and anionic comonomers in the polymer. PAM-based polybetaine copolymers typically contain sulfobetaine comonomers, such as 3-[(3-methacrylamidopropyl) dimethylammonio]propane-sulfonate, 3-[(2-methacryloxyethyl)dimethylammonio] propanesulfonate, and 3-[(2-acrylamido-2-methylpropyl)dimethylammonio] propanesulfonate[3,19,20,26] In the case of sulfobetaine copolymers with AM, the cationic and anionic charges are always equal in number because the charges are incorporated on the same mer unit. Many of these PAM-based PZs suffer from the effects of compositional drift during synthesis because of the differences in the reactivity of the (meth)acrylamido, methacrylic, and/or styrenic monomers, and the polymer products tend to be heterogeneous on the macromolecular level. However, McCormick and coworkers[24–26,28,33,34] showed that the effects of compositional drift are negligible when PAM-based PZs are prepared with only acrylamido monomers. In a recent study, Braun et al.[38] further validated this method of eliminating compositional drift by synthesizing polyampholyte terpolymers from *N*-isopropylacrylamide, NaAMPS, and (3-acrylamidopropyl)trimethylammonium chloride (APTAC). The terpolymers exhibited compositions close to that of the monomer feed at all degrees of conversion, and this indicated the formation of homogeneous terpolymer products.

There are relatively fewer studies of pH-responsive PAM-based PZs reported in the literature. McCormick and coworkers[2,24,28,39,40] have prepared several polyampholyte systems that demonstrate pH-triggerable changes in solution viscosity by utilizing (2-acrylamido-2-methylpropyl)dimethylammonium chloride (AMPDAC) or sodium 3-acrylamido-3-methylbutanoate (NaAMB) as pH-responsive comonomers with NaAMPS or AMPTAC, respectively. McCormick and Kathmann[33,34,36] examined copolymers of AM with various pH-responsive carboxybetaine comonomers; the copolymers exhibited pH-induced PZ-to-PE transitions leading to dramatic changes in the solution viscosity. Because of their unique combination of pH- and salt-responsive properties, these PAM-based PZs
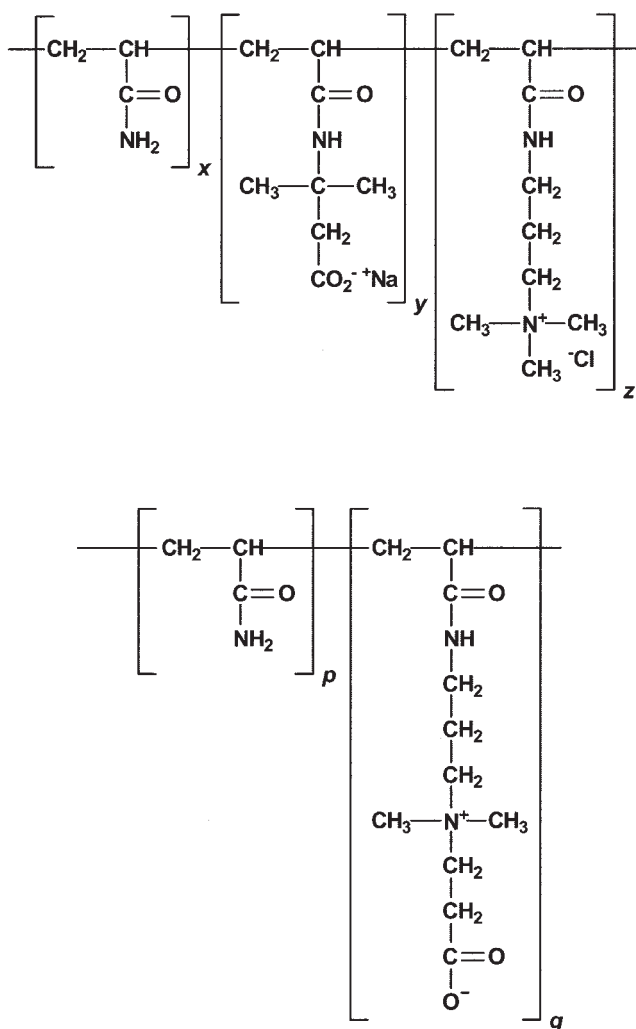
Figure 1 AMBATAC polyampholyte terpolymer and AM-DAP polybetaine copolymer.

represent an extremely interesting class of stimuli-responsive polymers that merit further investigation.

In the study reported here, a comparative analysis of pH-responsive PZs with polyampholyte or polybetaine architectures was conducted with well-defined model polymer systems of similar charge densities. The model PZs included polyampholyte terpolymers of AM, NaAMB, and APTAC and polybetaine copolymers of AM and 3-(3-acrylamidopropyldimethyl-ammonio)propionate (APDAP); the model PZs are called AMBATAC {poly[acrylamide-co-sodium 3-acrylamido-3-methylbutanoate-co-(3-acrylamidopropyl)-trimethylammonium chloride]} and AMDAP {poly-[acrylamide-co-3-(3-acrylamidopropyldimethylammo-nio) propionate]}, respectively (Fig. 1). The PZs were synthesized via free-radical solution polymerization in aqueous media, and the reactions conditions were selected to ensure that the terpolymers possessed random charge distributions, were homogeneous in composition, and did not have excessively broad molecu-

lar weight distributions (MWDs). The solution properties of the model PZs were investigated to elucidate the effects of the PZ architecture (i.e., polyampholyte vs polybetaine) on the stimuli-responsive solution behavior of these systems.

EXPERIMENTAL

Materials

All the chemicals were purchased from Aldrich and used as received, unless otherwise noted. β-Propiolactone (BPL) was purchased from Acros and used as received. 3-(N,N-dimethylamino)propylacrylamide (DMAPA) was distilled *in vacuo* and stored under N_2 before use. AM was recrystallized three times from acetone and dried *in vacuo* before use (mp = 83°C). 3-Acrylamido-3-methylbutanoic acid (AMBA) was synthesized according to the procedure of McCormick and Blackmon[41] and was recrystallized twice from methyl ethyl ketone before use (mp = 89–91°C). AP-DAP was synthesized via the quaternization of DMAPA with BPL according to the procedure of Liaw et al.[42] APDAP is extremely hygroscopic and was stored and handled only under an atmosphere of N_2. 2,2'-Azobis[2-(2-imidazolin-2-yl)propane] dihydrochloride (VA-044) was a gift from Wako Chemicals USA, Inc. (Richmond, VA), and was used as received. HCl and NaOH standard solutions (0.100 ± 0.005M) were purchased from Fisher Scientific (Pittsburgh, PA). Deionized (DI) water was obtained with a Barnstead Nanopure (Barnstead International, Dubuque, IA) reverse-osmosis/filtration unit (resistivity = 18.0 MΩ).

Synthesis of the AMBATAC polyampholyte terpolymers

Low-charge-density terpolymers of AM, NaAMB, and APTAC (denoted AMBATAC-Y-Z, where Y is the molar percentage of NaAMB and Z is the molar percentage of APTAC in the monomer feed) were synthesized via conventional free-radical polymerization in 0.5M NaCl. Sodium formate (NaOOCH) was added as a chain-transfer agent to control the polymer molecular weight (MW), suppress gel effects, and prevent excessive broadening of the MWD. The monomer concentration was held constant at 0.46M, and the ratio of the monomer concentration to the NaOOCH concentration was held constant at 32; this yielded terpolymer samples with weight-average molecular weights (M_w's) of 1–2 × 10^6 g/mol. The monomer-to-initiator ratio was 1000:1, and the reaction solution pH was adjusted to 8.5 ± 0.5 by the addition of NaOH to ensure the neutralization of the AMBA monomer to NaAMB. A typical polymerization procedure for AM-BATAC-5-5 is described next.

To a 2-L, three-necked, round-bottom flask equipped with a mechanical stirrer and an N_2 inlet/outlet were added degassed DI water (1500 mL) and NaCl (43.84 g, 0.750 mol). The flask was immersed in a 30°C constant-temperature bath, and the contents were sparged with N_2 for 20 min. AM (43.76 g, 0.616 mol), AMBA (5.86 g, 0.034 mol), APTAC (9.40 g of a 75 wt % APTAC solution in water, 0.034 mol), NaOH (1.40 g, 0.035 mol), and NaOOCH (1.45 g, 0.021 mol) were added to the flask, and stirring was allowed for 10 min. The pH of the monomer solution was adjusted to 8.5 ± 0.5 with 6.0M NaOH before the polymerization was initiated. VA-044 (221 mg, 0.684 mmol; dissolved in 10 mL of degassed DI water) was then added to the flask via syringe. The polymerization was allowed to proceed under an atmosphere of N_2 for 6.7 h. The stirring speed was adjusted to maintain a shallow vortex in the reaction medium. The reactor contents were discharged into Spectra-Por no. 4 dialysis tubing (Spectrum Laboratories, Rancho Dominguez, CA) (MW cutoff = 12–14,000 g/mol) and dialyzed against DI water for 1 week, the dialysis water being changed every 24–48 h. The pH of the dialysate was maintained at 7.25 ± 0.25 to ensure that the AMBA repeat units remained ionized. The purified terpolymer was isolated via lyophilization to yield a white, cottonlike solid. The conversion was determined gravimetrically.

Given the extremely hygroscopic nature of the AMBATAC terpolymers, it was desirable to obtain terpolymer samples with a higher bulk density and a lower surface area for ease of handling and solution preparation. Therefore, the lyophilized terpolymers were dissolved in DI water ([terpolymer] ≈ 10 wt %) and precipitated into absolute ethanol. The precipitated terpolymers were dried *in vacuo* at 50°C for 48–72 h and stored under N_2.

^{13}C-NMR: AMBATAC-5-5, NaAMB COO$^-$, 180.3, overlapping with AM C=O, 179.7 ppm; APTAC C=O, 177.2 ppm; NaAMB C=O, 175.5 ppm; APTAC quaternary ammonium CH_2, 64.4 ppm; APTAC quaternary ammonium CH_3, 53.3 ppm; NaAMB quaternary C, 52.8 ppm; APTAC amide CH_2, 48.6 ppm; NaAMB CH_2, 48.1 ppm; backbone CH, 42.1 ppm; backbone CH_2, 35.2 ppm; NaAMB *gem*-CH_3, 26.7 ppm; APTAC CH_2, 22.7 ppm. ^{1}H-NMR: AMBATAC-5-5, APTAC quaternary ammonium CH_2, 3.30 ppm; APTAC amide CH_2, 3.20 ppm; APTAC quaternary ammonium CH_3, 3.08 ppm, NaAMB CH_2, 2.47 ppm; backbone CH, 2.12–2.27 ppm; APTAC CH_2 1.97 ppm; backbone CH_2, 1.58–1.69 ppm; NaAMB *gem*-CH_3, 1.32 ppm.

Synthesis of the AMDAP polybetaine copolymers

Low-charge-density copolymers of AM and APDAP (AMDAP-Q, where Q is the molar percentage of APDAP in the monomer feed) were synthesized, puri-

fied, and isolated according to the same procedure used for the AMBATAC terpolymers, except that NaOH was not added to the monomer solution before initiation. The solution pH of the reaction medium was maintained at pH 7.0 ± 0.5 by the buffer action of NaOOCH.[43]

^{13}C-NMR: AMDAP-5, AM C=O, 179.6 ppm; APDAP COO$^-$, 177.1 ppm; APDAP amide C=O, 173.3 ppm; APDAP propionate quaternary ammonium CH_2, 62.4 ppm; APDAP propyl quaternary ammonium CH_2, 59.6 ppm; APDAP quaternary ammonium CH_3, 51.0 ppm; APDAP amide CH_2, 43.1 ppm; backbone CH, 42.3 ppm; backbone CH_2, 35.1 ppm; APDAP propionate CH_2, 27.8 ppm; APDAP propyl CH_2, 22.3 ppm. ^{1}H-NMR: AMDAP-5, APDAP propionate quaternary ammonium CH_2, 3.64 ppm; APDAP propyl quaternary ammonium CH_2, 3.40 ppm; APDAP amide CH_2, 3.33 ppm; APDAP quaternary ammonium CH_3, 3.16 ppm; APDAP propionate CH_2, 2.88 ppm; APDAP propyl CH_2, 2.74 ppm; backbone CH, 2.08–2.40 ppm; backbone CH_2, 1.70–1.83 ppm.

Polymer characterization

NMR spectroscopy

The samples for NMR spectroscopy analysis were prepared as 5–10 wt % solutions in D_2O containing 0.5M NaCl. All the NMR experiments were performed at the ambient temperature (25.0 ± 1.0°C). ^{13}C-NMR spectra for the polymers were obtained at 125 MHz with a Varian Unity-Inova NMR spectrometer (Varian, Inc., Palo Alto, CA) with a standard 5-mm, two-channel probe. For the quantitative determination of the polymer composition, a gated decoupled pulse sequence with a 6–7 s relaxation delay was used to suppress nuclear Overhauser effects. Typically, 10,000–15,000 scans were accumulated for the ^{13}C spectra. All shifts were referenced automatically by the acquisition software (VNMR version 6.1C) with a resonance frequency of D_2O. The error associated with individual values of monomer incorporation determined via the integration of ^{13}C-NMR signals was generally ±5% of the value. ^{1}H-NMR spectra were obtained at 300 MHz on a Varian Mercury Plus spectrometer. Typical acquisition parameters were a relaxation delay of 0.05 s, a 7.1-μs pulse corresponding to a 90° flip angle, and an acquisition time of 2 s. Data analysis was performed with MestRe-C (version 2.3a) spectral analysis software (Departamento de Química Orgánica, Universidad de Santiago de Compostela A Coruña, Spain).

Elemental analysis

Elemental analysis for Na$^+$ and Cl$^-$ was performed by Bonner Analytical Testing Co. (Hattiesburg, MS). The

samples of the polymers were analyzed to determine the content of residual counterions remaining after purification via dialysis.

Size exclusion chromatography/multi-angle laser light scattering (SEC–MALLS)

Aqueous size exclusion chromatography (SEC) was used to determine the polymer MW, radius of gyration (R_g), and polydispersity index (PDI). The SEC system consisted of an Agilent 1100 series isocratic pump with a vacuum degasser (Agilent Technologies, Palo Alto, CA), a Rheodyne 7725i manual injector (Rheodyne LLC, Rohnert, CA) with a 100-μL injection loop, two Viscogel columns (GPW$_{XL}$ 5000 and 6000 and a GPW$_{XL}$ guard column, Viscotek) connected in series, a EOS 18-angle laser light scattering detector (Wyatt Technologies), and an Optilab DSP interferometric refractometer (Wyatt Technologies, Santa Barbara, CA). The data acquisition and analysis were performed with chromatography software (Wyatt Technologies). SEC analysis was conducted at the ambient temperature ($25.0 \pm 1.0°C$). The eluent used for SEC analysis of the polymers was a 0.1-μm-filtered 0.1M NaCl phosphate buffer (pH 7; 25 mM NaH$_2$PO$_4$ and 25 mM Na$_2$HPO$_4$). Refractive-index (RI) increments (dn/dc) of the PZs were determined with the refractometer in the offline mode at the ambient temperature. dn/dc values determined offline was typically $\pm$2–3%. The SEC–MALLS data reported are the averages of three separate injections. The error associated with individual values of M_w determined via SEC–MALLS was typically less than or equal to $\pm$2%.

Potentiometric titration

The pH measurements for potentiometric titrations were conducted at $25.0 \pm 0.5°C$ with an Orion 900A pH meter with a Ross Sure-Flow 8175 pH electrode (Thermo Electron, Waltham, MA). The meter was calibrated via a two-point calibration method. The polymer concentrations (c) for titration were 0.50 g/dL; minimal volume variation during titration was achieved by the addition of microliter aliquots of the titrant. Polymer solutions were adjusted to pH $\sim$ 10 with concentrated NaOH to ensure the complete neutralization of all carboxylic acid groups and then were back-titrated with a 0.1M HCl standard solution.

Solution rheological analysis

Sample preparation

Stock solutions were prepared through the dissolution of vacuum-oven-dried polymer samples in DI water or saline media; these were allowed to age 48–72 h while agitating gently on an orbital shaker. Dilutions of the stock solutions were prepared with DI water or saline media, accordingly. The samples were allowed to age overnight on an orbital shaker before analysis. The adjustment of the pH was achieved via the addition of microliter aliquots of concentrated NaOH or HCl. The adjustment of the pH was performed on the same day as the rheological analysis to prevent acid- and base-catalyzed hydrolysis of the AM repeat units upon aging at pH extremes. The solution pH was measured before the sample analysis with a Check-Mite pH-20 pH meter (Corning).

Dilute-solution viscometry

The apparent viscosities (η_{app}) of dilute polymer solutions were determined with a Contraves LS-30 low-shear rheometer with the 2T cup and bob geometry, operating at 5.96 s^{-1} and 25°C. Dilute-solution η_{app} values were initially measured at various shear rates, and the solutions were observed to be Newtonian fluids (i.e., non-shear-thinning); thus, the η_{app} values determined at 5.96 s^{-1} were considered to be zero-shear η_{app} values. The measurements of η_{app} were repeatable with a precision of $\pm$1%. The specific viscosity (η_{sp}) was calculated from η_{app} (cP):

$$\eta_{sp} = \left(\frac{\eta_{app} - \eta_o}{\eta_o} \right) \tag{1}$$

where η_o is the solvent viscosity (cP). The reduced viscosity (η_{red}; dL/g) was calculated by the division of η_{sp} by c (g/dL) The intrinsic viscosities ([η]) were determined by the plotting of η_{red} versus c and extrapolation to zero concentration. The determinations of [η] were repeatable to within $\pm$2%.

RESULTS AND DISCUSSION

PZ terpolymer and copolymer synthesis

Figure 1 depicts the structures of the model PZs synthesized for this study. The primary goal of this study was to elucidate the effects of the charge placement in low-charge-density PZs (i.e., on separate repeat units in polyampholytes vs on the same repeat unit in polybetaines); thus, monomer feed compositions were selected to yield polyampholytes and polybetaines that contained equal numbers of formal charges. PZ compositions containing a minimum of 80 mol % AM were targeted to yield PZs with high solubility and good viscosifying properties. NaAMB and APDAP were selected as comonomers primarily because of their pH-responsive nature (i.e., COO$^-$ functionality). However, NaAMB also possesses several other features that make it a highly desirable monomer for applications in salt-responsive viscosifiers, including increased hydrolytic stability, greater steric bulk (lead-

TABLE I
Conversion and Compositional Data for the Synthesis of AMBATAC Terpolymers and AMDAP Copolymers

Sample	Reaction time (h)	Conversion (%)[a]	AM (mol %)[b]	NaAMB (mol %)[b]	APTAC (mol %)[b]	APDAP (mol %)[b]
Polyampholyte						
AMBATAC-5-5	6.7	79	91.4	4.6	4.3	—
AMBATAC-10-10	8.0	78	77.9	10.8	11.3	—
Polybetaine						
AMDAP-5	6.8	87	96.0	—	—	4.0
AMDAP-10	6.8	91	90.4	—	—	9.6

[a] Conversion determined gravimetrically.
[b] Determined via inverse-gated decoupled ^{13}C-NMR spectroscopy.

ing to increased polymer chain stiffness), and out-standing resistance to divalent ion binding (preventing polymer phase separation in hard brines).[41,44–46] APTAC, a non-pH-responsive quaternary ammonium acrylamido monomer, was used as the cationic monomer in the AMBATAC series. APTAC is commercially available and was selected for this work because of the complexity associated with synthesizing (three-step synthetic procedure) and purifying (high tendency for autopolymerization) the AMPTAC monomer used in previous studies.[28,47] APDAP was chosen because of its structural similarity to APTAC and ease of preparation: APDAP is readily synthesized from commercially available DMAPA and BPL via a one-step quaternization reaction.[42]

The monomers and reaction conditions used in the synthesis of the model PZs were chosen to yield systems with homogeneous compositions, random charge distributions, and well-defined MWs and MWDs. McCormick and coworkers[23–26,28,33,34] showed that the effects of compositional drift are negligible when only acrylamido monomers are used in the synthesis of PAM-based PZs (because of the similar reactivities of the acrylamido polymerizable groups). Hence, AMBATAC and AMDAP polymerizations can be carried out to relatively high conversions (>75%) while maintaining relatively homogeneous terpolymer and copolymer compositions. To ensure the random distribution of the ionic and zwitterionic monomers along the terpolymer chain, the model PZs were synthesized in 0.5M NaCl. The addition of NaCl to the reaction medium screens the electrostatic interactions between charged monomers; thus, the tendencies for the charged monomers to be incorporated into the polyampholyte terpolymers as alternating pairs and into the polybetaine copolymers as blocky segments are greatly reduced.[21,26,33,34,48] In previous studies of PAM-based PZs synthesized by free-radical polymerization, the degrees of polymerization (DPs) were observed to vary widely, depending strongly on the monomer feed compositions.[24,25,28,33,34,36,49] To eliminate the effects of the monomer feed composition on DP, the polymerizations in this study were conducted in the presence of NaOOCH as a chain-transfer agent. NaOOCH is highly

effective in controlling MW and suppressing broad MWDs in the polymerization of acrylamido monomers.[50] Additionally, the polymerizations were conducted slightly above room temperature (30°C) to minimize chain branching and hydrolysis reactions, which can occur at higher temperatures.[51–53]

The first column in Table I indicates the target compositions of the model PZs synthesized for this study (AMBATAC-Y-Z, where Y is the molar percentage of NaAMB and Z is the molar percentage of APTAC in the monomer feed, and AMDAP-Q, where Q is the molar percentage of APDAP; the balance of both monomer feeds is composed of AM). Charge-balanced AMBATAC terpolymers containing 10–20 mol % total ionic comonomer and APDAP copolymers containing 5–10 mol % zwitterionic comonomer were prepared, corresponding to equal charge densities in the AMBATAC-5-5 and AMDAP-5 and AMBATAC-10-10 and AMDAP-10 systems, respectively. The polymerizations were conducted for 6–8 h to obtain conversions of approximately 80–90%. Table I shows that longer reaction times were required to reach high conversion for the AMBATAC terpolymers. This is attributed to the presence of the hydroquinone monomethyl ether retarder present in the commercially available APTAC monomer, which leads to longer induction periods as the level of APTAC in the feed is increased.

Compositional analysis

The terpolymer and copolymer compositions were determined via inverse-gated decoupled ^{13}C-NMR spectroscopy, which allowed for the quantitative integration of the signals in the ^{13}C spectra. The model PZ compositions determined via NMR spectroscopy (Table I) are in very good agreement with the target compositions, deviating less than 1.0 mol % from the targeted values.

It has been established that the purification of polyampholytes via exhaustive dialysis against DI water leads to self-neutralization of the polyampholyte, in which the polymer-bound cations and anions pair with each other as the mobile counterions diffuse
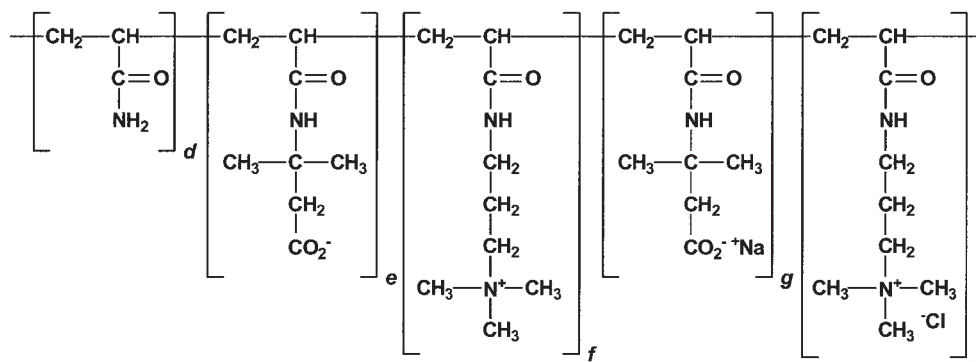
Figure 2 Composition of AMBATAC terpolymers after purification via dialysis.

away from the polymer.[30,40,54] Self-neutralization can occur intramolecularly and intermolecularly. Thus, after purification via dialysis, the bulk compositions of the AMBATAC terpolymers are best represented by the structure in Figure 2, which consists of *d* AM repeat units, *e* + *f* AMB–APTA repeat unit pairs, and *g* NaAMB and/or *h* APTAC repeat units that still bear counterions. With the compositional data in Table I, the maximum number of AMB–APTA (AMB = 3-acrylamido-3-methylbutanoate; APTA = (3-acrylamidopropyl)trimethylammonium) repeat unit pairs was calculated assuming 100% charge pairing of the charged repeat unit present in the least content (Table II). The excess charged repeat units were assumed to retain their counterions to maintain the charge neutrality of the system. To verify the terpolymer compositions presented in Table II, samples of the terpolymers were analyzed for residual sodium (Na^+) and chloride (Cl^-) contents. Under the assumption that each ionic repeat unit bears a counterion, the maximum theoretical Na^+ and Cl^- contents before dialysis and self-neutralization can be estimated from the compositional data in Table I. If no self-neutralization occurred in the AMBATAC-5-5 and AMBATAC-10-10 terpolymers, then the terpolymers would be expected to contain 1.3–2.5 wt % Na^+ and 1.9–4.0 wt % Cl^- (Table III). After the dialysis and charge pairing of ionic monomers, the residual counterion contents due to the presence of excess ionic repeat units can be estimated with the compositional data in Table II, assuming 100% self-neutralization of the charged repeat unit present in the least content. The results of the elemental analysis for Na^+ and Cl^- agree well with

the expected values, indicating that the AMBATAC terpolymers are indeed highly self-neutralized and only bear counterions on ionic repeat units present in excess of the oppositely charged repeat units.

Because each APDAP monomer unit contains an anionic charge and a cationic charge, the zwitterionic repeat units exist as self-neutralized species or inner salts.[5,55] Thus, the AMDAP copolymers are not expected to retain mobile counterions upon purification via dialysis. Elemental analysis revealed that the AMDAP copolymers did not contain any residual Na^+ or Cl^- (Table III), confirming complete self-neutralization of the APDAP repeat units and complete NaCl removal upon purification via dialysis.

SEC–MALLS analysis

MW, R_g, and PDI data for the model PZs were obtained via SEC coupled with multi-angle laser light scattering (MALLS) and RI detection. SEC was performed with a $0.1M$ NaCl phosphate buffer (pH 7) as the eluent to ensure the solubility of the PZs and to suppress intermolecular aggregation. When used in conjunction with dn/dc values determined offline (Table IV), MALLS detection enables the determination of the absolute MWs without the necessity of polymer standards and universal calibration techniques. The results of a typical SEC–MALLS analysis are shown in Figure 3 for AMDAP-10, where the RI response and MW of each chromatogram slice are plotted as a function of the elution volume. The RI signal indicates a unimodal MWD with a low-MW tail; this MWD is characteristic of high-conversion PAM products syn-

TABLE II
Compositional Data for Dialyzed AMBATAC Terpolymers

Sample	AM (*d*; mol %)	AMB–APTA pairs (*e* + *f*; mol %)	NaAMB (*g*; mol %)	APTAC (*h*; mol %)
AMBATAC-5-5	91.1	4.3	0.3	0.0
AMBATAC-10-10	77.9	10.8	0.0	0.5

TABLE III
Residual Counterion Content in the AMBATAC Terpolymers and AMDAP Copolymers

Sample	Na$^+$, predialysis (wt %)[a]	Cl$^-$, predialysis (wt %)[a]	Na$^+$, postdialysis (wt %)[b]	Cl$^-$, postdialysis (wt %)[b]	Na$^+$, found (wt %)[c]	Cl$^-$, found (wt %)[c]
Polyampholytes						
AMBATAC-5-5	1.3	1.9	0.1	0.0	0.1	ND[d]
AMBATAC-10-10	2.5	4.0	0.0	0.2	<0.1	0.2
Polybetaines						
AMDAP-5	—	—	—	—	ND	ND
AMDAP-10	—	—	—	—	ND	ND

[a] Theoretical value calculated from ^{13}C-NMR compositional data with the assumption that each ionic repeat unit bears a counterion.
[b] Theoretical value calculated from ^{13}C-NMR compositional data with the assumption that the repeat unit present in the least content is completely self-neutralized.
[c] Determined via elemental analysis.
[d] ND = not detected.

thesized in the presence of NaOOCH as a chain-transfer agent.[50] The negatively sloped linear decrease in MW as a function of the elution volume indicates very good separation of the various MW fractions in the polydisperse sample by size exclusion. The scatter of MW data points observed at higher elution volumes (as the RI signal returns to the baseline, indicating c > 0 at these elution volumes) indicates that the polymer is not being retained on the SEC columns because of polymer–column affinity and/or overloading of the columns. The mass recovery of injected polymer samples was typically greater than or equal to 90 wt % as determined by RI detection.

Table IV lists the values of M_w, PDI, and R_g for the model PZs. The M_w values of the model PZs range from 1.4 to 1.5×10^6 g/mol, corresponding to DPs of $1.6–1.9 \times 10^4$ repeat units. Figure 4 shows the MWDs of the model PZs. The AMBATAC terpolymers exhibit unimodal MWDs of similar shape, with PDI values of 1.51 and 1.65 for AMBATAC-5-5 and AMBATAC-10-10, respectively. The MWDs of the AMDAP-5 and AMDAP-10 copolymers are slightly broader, with PDIs of 2.03 and 2.11, respectively; nonetheless, the

peak values of M_w and DP for the model PZs fall in a relatively narrow range. The broader MWDs observed in the AMDAP copolymers can be attributed to the higher conversions of the AMDAP polymerizations, as PDIs tend to increase with conversion when NaOOCH is used as a chain-transfer agent.[50] Overall, these data indicate that the use of NaOOCH in the synthesis of the model PZs is effective at eliminating the effects of the monomer feed composition on DP and maintaining PDIs less than or equal to 2.1 by suppressing gel effects. Weight-average values of R_g in the SEC eluent (Table IV) are slightly higher for the AMBATAC terpolymers (66–67 nm) than for the AMDAP terpolymers (61–63 nm), although the polymers have similar DPs. The values of R_g for the AMBATAC terpolymers are most likely higher because of the lower PDIs of the terpolymer samples.

Relationship of the radius of gyration to the molecular weight (R_g–M)

Because SEC–MALLS analysis provides an R_g value for each slice of the chromatogram, the technique en-

TABLE IV
SEC–MALLS Analytical Data for AMBATAC Terpolymers and AMDAP Copolymers

Sample	dn/dc (mL/g)[a]	M_w (10^6 g/mol)[b]	PDI[b]	R_g (nm)[b,c]	DP $\times 10^{-4}$[d]
Polyampholytes					
AMBATAC-5-5	0.1737	1.51	1.51	65.7	1.90
AMBATAC-10-10	0.1861	1.52	1.65	66.5	1.63
Polybetaines					
AMDAP-5	0.1707	1.43	2.03	61.3	1.85
AMDAP-10	0.1659	1.43	2.11	62.7	1.82

[a] Determined in a 0.1M NaCl phosphate buffer (pH 7) at 25 ± 0.5°C.
[b] Determined via aqueous SEC–MALLS in a 0.1M NaCl phosphate buffer (pH 7).
[c] R_g = weight-average radius of gyration.
[d] DP = weight-average degree of polymerization, calculated from M_w and ^{13}C-NMR compositional data.
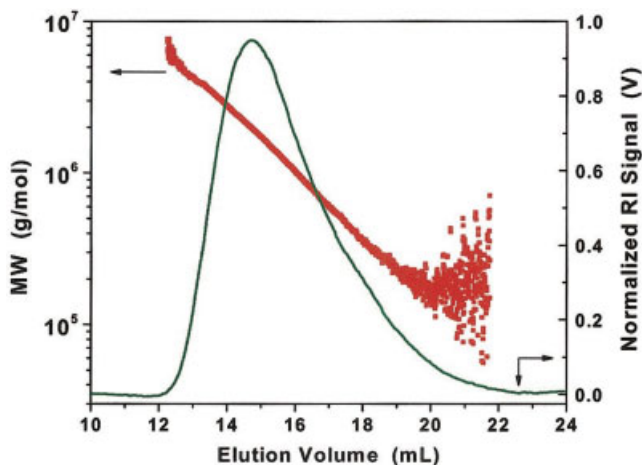
Figure 3 SEC–MALLS–RI data for AMDAP-10 in a 0.1M NaCl phosphate buffer (pH 7).

ables an examination of the relationship between R_g and MW:

$$R_g = K_{R_g}M^\rho \tag{2}$$

where M is the polymer MW and K_{R_g} and ρ are the intercept and slope of a log–log plot of R_g versus M, respectively. ρ reveals how the mass of the polymer fills space and is indicative of the macromolecular conformation in solution.[56] The theoretical slopes for hard spheres, random coils at θ conditions, random coils in good solvents, and rigid rods are 0.33, 0.50, 0.55–0.60, and 1.0, respectively. An examination of the ρ values in Table V reveals that AMBATAC-5-5, AMDAP-5, and AMDAP-10 exist as a random coils with no excluded volume in a 0.1M NaCl phosphate buffer (pH 7), whereas AMBATAC-10-10 adopts a slightly collapsed conformation ($\rho = 0.46$ for AMBATAC-10-10). This observation implies that there is a net nega-
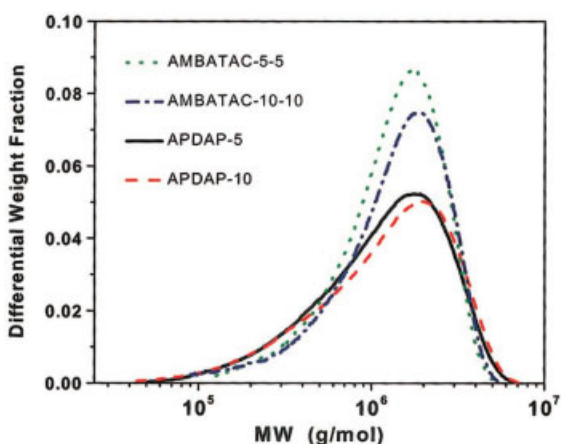

Figure 4 MWDs of the AMBATAC terpolymers and AMDAP copolymers.

TABLE V
Coefficients of the R_g–M Relationship Determined via SEC–MALLS

Sample	K_{R_g} [10^2 nm^{-1} (g/mol)$^{-\rho}$][a]	ρ[a]
Polyampholytes		
AMBATAC-5-5	6.08	0.50
AMBATAC-10-10	11.5	0.46
Polybetaines		
AMDAP-5	5.03	0.50
AMDAP-10	5.12	0.50

[a] Determined via aqueous SEC–MALLS in a 0.1M NaCl phosphate buffer (pH 7).

tive excluded-volume effect in the higher charge density AMBATAC-10-10 because of unscreened electrostatic attractions and/or greater hydrophobicity of the uncharged portion of the polymer backbone. The values of the pre-exponential term, K_{R_g}, are lower for the AMDAP copolymers, indicating that the polybetaine copolymers possess greater conformational freedom than the polyampholyte terpolymers.

Relationship of [η] to the MW

The [η] value of an unperturbed polymer coil in solution (i.e., at or near θ conditions, under which excluded-volume effects are minimal) is related to the MW and R_g of the coil by the Flory–Fox relationship:

$$[\eta] = 6^{\frac{3}{2}}\Phi_0\frac{(R_g)^3}{M} \tag{3}$$

where M is the MW of the polymer and Φ_0 is the Flory viscosity constant.[57,58] Because the R_g–M relationships for the model PZs revealed that the polymers did not exhibit significant excluded-volume effects under the given SEC conditions, the Flory–Fox relationship was used to determine the PZ [η] values from the R_g and MW at each point on the SEC chromatogram (Flory constant values have been reported to range from 1.81 to 2.87 $\times$ 10^{23} mol^{-1}; for this work, the Hearst–Tagami asymptotic value of Φ_0 for non-free-draining, linear, flexible chains of high DP was used: 2.19 $\times$ 10^{23} mol^{-1}.[57]) The intrinsic viscosities of the unfractionated PZ samples determined via SEC–MALLS ([η]$_{SEC}$) were calculated as follows:

$$[\eta]_{SEC} = \frac{\sum_i ([\eta]_i c_i)}{\sum_i c_i} \tag{4}$$

where [η]$_i$ is the intrinsic viscosity of chromatogram slice i (dL/g) and c_i is the polymer concentration (determined via RI detection) of chromatogram slice i

<div align="center">

TABLE VI
Viscometric and SEC–MALLS Data for the $[\eta]$–M Relationship of the AMBATAC Terpolymers and AMDAP Copolymers

</div>

Sample	$[\eta]_{SEC}$ (dL/g)[a]	$[\eta]$ (dL/g)[b]	k_H[b]	K_{MHS} $[10^3 \text{ dL/g (g/mol)}^{-a}]$[c]	a[c]	a (calculated)[d]
Polyampholytes						
AMBATAC-5-5	5.57	5.14	0.43	4.43	0.50	0.50
AMBATAC-10-10	5.67	5.09	0.47	9.67	0.44	0.38
Polybetaines						
AMDAP-5	4.75	4.72	0.25	2.26	0.53	0.50
AMDAP-10	4.80	4.45	0.28	2.57	0.52	0.50

[a] Determined with the Flory–Fox relationship and SEC–MALLS data.
[b] Determined in a 0.1M NaCl phosphate buffer (pH 7) at 25°C and 5.96 s^{-1}.
[c] Determined via aqueous SEC–MALLS in a 0.1M NaCl phosphate buffer (pH 7).
[d] Calculated with the ρ value from the R_g–M relationship.

(g/dL). The values of $[\eta]_{SEC}$ determined for AMBATAC-5-5 and AMBATAC-10-10 were 5.57 and 5.67 dL/g, respectively (Table VI). AMDAP-5 and AMDAP-10 exhibited slightly lower $[\eta]$ values (4.75 and 4.80 dL/g, respectively), most likely because of the broader MWDs of the polybetaines. To verify that the $[\eta]_{SEC}$ values and Flory–Fox relationship were correct, we measured the $[\eta]$ values of the AMBATAC terpolymers in the SEC eluent via low-shear dilute-solution viscometry at 25°C (Table VI). The values of $[\eta]_{SEC}$ and $[\eta]$ determined by viscometry were in agreement, although the $[\eta]$ values determined by the latter technique tended to be slightly lower (7–10%) than the $[\eta]_{SEC}$ values. These differences may be attributed to errors in the viscometry sample concentrations due to water present (despite exhaustive drying) in the weighed polymers. SEC–MALLS with RI detection is not susceptible to errors due to associated water, as the RI detector only detects the mass of the polymer present in a given sample. Overall, the $[\eta]$ data obtained by different methods agree, indicating the utility of the Flory–Fox relationship to calculate $[\eta]_{SEC}$.

Table VI also lists values of the Huggins constant (k_H) for the model PZs in the SEC eluent, as determined via dilute-solution viscometry. The k_H data provide additional information on polymer–solvent interactions and macromolecular conformation and correlate well with the R_g–M relationship data in Table V. k_H ranges from 0.43 to 0.47 for the AMBATAC terpolymers; such k_H values are characteristic of polymers that are at or slightly below θ conditions.[59] However, the AMDAP copolymers exhibit k_H values of 0.25–0.28, which indicate more favorable polymer–solvent interactions and greater conformational freedom in these systems.

The Mark–Houwink–Sakurada (MHS) relationship [eq. (5)] relates $[\eta]$ of a polymer coil in solution to the MW of the polymer; the coefficients K_{MHS} and a are determined from a log–log plot of $[\eta]$ versus M.[59] Like the R_g–M relationship, the MHS relationship provides information about the properties of macromolecules in

solution that are correlated to the macromolecular structure and polymer–solvent interactions:

$$[\eta] = K_{MHS}M^a \tag{5}$$

With the MW and $[\eta]_{SEC}$ data, MHS parameters (i.e., K_{MHS} and a) for the model PZs in a 0.1M NaCl phosphate buffer (pH 7) at 25°C were determined (Table VI). The $[\eta]_i$ values were plotted as a function of the MW of each slice (M_i) to yield MHS plots. An examination of the MHS parameters listed in Table VI reveals that the a values for the AMDAP copolymers are greater than those of the AMBATAC terpolymers, suggesting the polybetaines adopt more open, random conformations with greater excluded volume than the polyampholytes under SEC conditions. The lower values of K_{MHS} for the AMDAP copolymers indicate that increased polymer–solvent interactions and greater conformational mobility occur in the polybetaine systems. The data in Table VI also show that the values of a decrease and the values of K_{MHS} increase as the charge density of the PZs is doubled; however, the magnitude of the change in the K_{MHS} and a values as a function of the charge density is much greater in the AMBATAC polyampholytes. This indicates that the electrostatic interactions between the oppositely charged AMB and APTA units in the polyampholytes are much stronger than the interactions between the zwitterionic APDAP units in the polybetaines.

The MHS a value is related to the ρ value of the R_g–M relationship by eq. (6), which is derived from the Flory–Fox theory.[57] To verify the applicability of the Flory–Fox equation to the model PZ systems, values of a were calculated from the ρ values in Table V. Overall, the calculated values of a (Table VI) agree with the experimentally determined a values. However, the calculated (i.e., Flory–Fox) a value for AMBATAC-10-10 ($a_{calc} = 0.38$) is significantly lower than the experimental value ($a_{expt} = 0.44$). This deviation may be attributed to negative excluded-volume effects (collapse due to unscreened electrostatic attractions

and increased backbone hydrophobicity) that occur for AMBATAC-10-10 under SEC conditions:

$$a = (3\rho) - 1 \qquad (6)$$

Potentiometric titration

Potentiometric titrations of the model PZs in DI water were conducted to determine the apparent pK_a values for the COOH groups on the AMB and APDAP repeat units. The AMBATAC terpolymers exhibit significantly higher apparent pK_a values than the AMDAP copolymers, and this indicates the increased acidity of the APDAP COOH group in comparison with the AMB COOH group. The lower values of apparent pK_a observed for the polybetaines are due to the influence of the positive field of the quaternary ammonio substituent on the basicity of the COO$^-$ group.[5,55] Protonation of the COO$^-$ group is less favorable for the APDAP units because of the close proximity of the ammonio group to the COO$^-$ group (i.e., as both groups are on the same repeat unit); therefore, pK_a of the conjugate acid is lower. In the case of the AMBATAC terpolymers, AMB COO$^-$ groups are located significantly farther away from the positively charged APTA moieties (i.e., on separate repeat units). Because the APDAP COO$^-$ groups are less attractive to protons than the AMB COO$^-$ groups, the AMBATAC terpolymers exhibit greater values of the apparent pK_a. The apparent pK_a values of the model PZs also increase as the charge density is doubled, and this indicates that the PZs become less acidic as the charge density is increased; this phenomenon is similar to that observed by McCormick and Elliot[46] for copolymers of AM with NaAMB. The magnitude of the increase is greater in the polyampholytes than in the polybetaines, and this indicates that the charge-density effects on the apparent pK_a values are stronger in the polyampholytes. The effects of the charge density are stronger in the polyampholytes because the spacing between anionic and cationic groups changes more dramatically with increasing comonomer incorporation (i.e., with increasing charge density, there are fewer AM repeat units separating AMB and APTA units than AM repeat units separating APDAP units). In addition, the charge spacing in the polyampholytes is determined solely by the comonomer sequence distribution, whereas the charge spacing in the polybetaines is determined primarily by the length of the ion bridge (i.e., the number of methylene spacer units between the ammonio and carboxylate groups) and by the comonomer sequence distribution.

Polymer solubility

The solubility of the model PZs in DI water was examined at both semidilute (c = 2.0 g/dL) and dilute (c

TABLE VII
Apparent pK_a Values for the AMBATAC Terpolymers and AMDAP Copolymers

Sample	Apparent pK_a of the COOH group[a]
Polyampholytes	
AMBATAC-5-5	5.13
AMBATAC-10-10	5.73
Polybetaines	
AMDAP-5	4.24
AMDAP-10	4.57

[a] Determined in DI water at 25°C.

= 0.1 g/dL) concentrations. The ambient pH of model PZ solutions in DI water is typically 6.5 ± 0.2, corresponding to degrees of AMB unit ionization of 90% or more and degrees of APDAP ionization of 99% or more for the AMBATAC terpolymers and AMDAP copolymers, respectively (based on the apparent pK_a values listed in Table VII). The AMDAP copolymers exhibit the greatest solubility in DI water, yielding totally transparent solutions under dilute and semidilute conditions. The polybetaines also dissolve faster than the polyampholytes. AMBATAC-5-5 has excellent solubility in DI water, yielding transparent solutions at dilute concentrations and transparent solutions with a slight haze under semidilute conditions. Semidilute-solutions of AMBATAC-10-10 are also transparent, yet they are hazier than the AMBATAC-5-5 solutions. The increased haziness of the AMBATAC-10-10 solution is most likely caused by microaggregates of oppositely charged repeat units that scatter light. At dilute concentrations, AMBATAC-10-10 is readily dispersible in DI water under gentle mixing, yielding hazy, yet exceedingly translucent, solutions. When a dilute AMBATAC-10-10 solution is left to stand for long periods of time (1–2 weeks), phase separation can be observed, with two transparent layers forming in the solution. Upon gentle mixing, the lower phase is readily dispersed into the upper phase, the resulting solution having the appearance of the initial AMBATAC-10-10 solution.

The solubility of the model PZs is readily explained in terms of charge placement. The incorporation of the cationic and anionic charges as zwitterionic APDAP units in the polybetaines yields a copolymer architecture of dipolar functionalities connected by long runs of nonionic AM. The dipolar nature of the carboxybetaine groups renders the polybetaines extremely hydrophilic with excellent solubility in the absence of electrolytes.[5,6,35,42,55,60–62] Although charge-balanced polyampholyte copolymers precipitate at the solution isoelectric point (IEP; i.e., pH at which the number of anionic groups and the number of cationic groups are equal),[6] polycarboxybetaines remain soluble at the solution IEP. The solubilities of the model PZs indicate
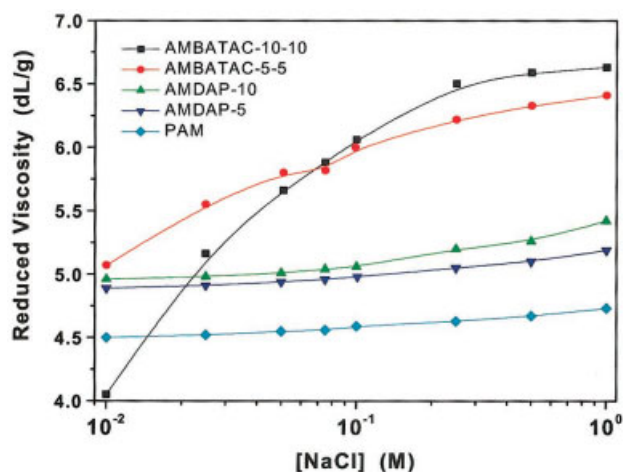
Figure 5 η_{red} as a function of the NaCl concentration for the AMBATAC terpolymers and AMDAP copolymers at the ambient pH (6.5 ± 0.2). The data for a PAM homopolymer with a similar DP (1.94×10^4 repeat units) are shown for comparison ($c = 0.1$ g/dL).

that the dipolar electrostatic attractions between zwitterionic APDAP units in the polybetaines are weaker than the ionic electrostatic attractions between AMB and APTA units in the polyampholytes (i.e., the AMB and APTA units are discrete cationic and anionic species). The phase separation observed in AMBATAC-10-10 is further evidence for stronger intramolecular and intermolecular associations in the polyampholyte in comparison with a highly soluble polybetaine of similar charge density, AMDAP-10. Although the polymer–polymer interactions are stronger in the AMBATAC terpolymers, the high levels of hydrophilic AM comonomer and slight charge imbalances impart solubility to the polyampholytes, albeit to a lesser degree than AMDAP copolymers of a similar charge density.

Salt-responsive solution viscosity

Figure 5 shows the dilute-solution ($c = 0.1$ g/dL) η_{red} values of the model PZs as a function of the NaCl concentration; η_{red} of a nonionic PAM homopolymer of a comparable DP (DP $= 1.94 \times 10^4$ repeat units) is also shown for comparison. The solution viscosities of the PZs increase with increasing NaCl concentration, indicating antipolyelectrolyte behavior; however, the magnitude of the viscosity change is much greater for the polyampholytes. The more dramatic salt response of the AMBATAC terpolymers indicates that the intramolecular forces being screened by the added electrolyte are much greater in the polyampholytes than in the polybetaines, which only exhibit mild antipolyelectrolyte effects despite having similar charge densities. The increased chain stiffness caused by the incorporation of the bulky AMB units in the AMBATAC

terpolymers also contributes to the higher solution viscosities observed for the polyampholytes with increasing NaCl concentration. McCormick and coworkers[63–65] showed that NaAMB and other structurally similar acrylamido monomers cause chain stiffening when incorporated at low levels into copolymers with AM. The increased chain stiffness is due to the interaction of the AMB repeat units with adjacent AM units, which forms hydrogen-bonded ring structures along the polymer backbone. Such effects are operative in the AMBATAC terpolymers and absent in the AMDAP copolymers. A careful examination of Figure 5 also reveals that uncharged PAM shows a small increase in η_{red} with increasing NaCl concentration, and this indicates greater polymer–solvent interactions with increasing ionic strength. Munk et al.[66] also showed that PAM exhibits increased polymer–solvent interactions in aqueous solutions with increasing NaCl concentration. Thus, the antipolyelectrolyte effects in the model PZs are actually enhanced because of the high AM content of these low-charge-density systems.

**pH-responsive solution viscosity**

In the absence of electrolytes

Figure 6 shows dilute-solution ($c = 0.1$ g/dL) η_{red} values as a function of the solution pH for the model PZs in DI water. In the absence of added electrolytes, the PZs exhibit the most profound pH response because electrostatic interactions can occur over very long ranges in the salt-free solutions (i.e., charge screening is virtually nonexistent). The AMBATAC terpolymers exhibit similar pH-responsive behavior, although the magnitude of the observed behavior is greater for the higher charge density terpolymer (AMBATAC-10-10). At a low solution pH (2–3.5), the AM-
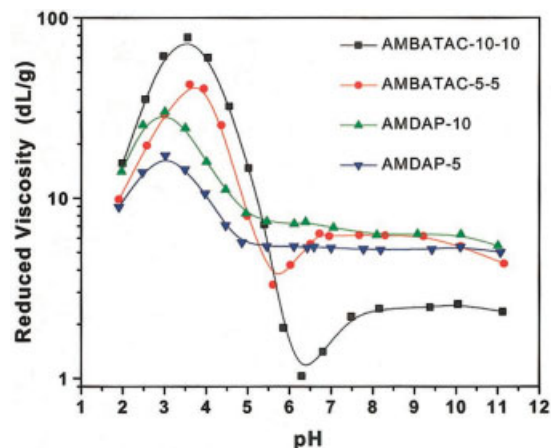
Figure 6 η_{red} of the AMBATAC terpolymers and AMDAP copolymers in DI water as a function of the solution pH ($c = 0.1$ g/dL).

BATAC terpolymers exist as cationic PEs because of protonation of the AMB COO^- groups. Below pH 3.5, a distinct PE effect can be observed: the extended PE coils undergo conformational contraction because of the increasing ionic strength of the medium as HCl is added to lower the solution pH. As the solution pH increases from 3.5 to 7, the AMB units are neutralized, triggering PZ behavior and the collapse of the terpolymer coils because of electrostatic attraction. The minima in the pH traces for each terpolymer correspond to the solution IEPs. The observed solution IEPs represent the average IEP for all terpolymers in solution, and the IEP of individual terpolymer molecules in a given sample is likely to occur over a small pH range because of the polydispersity of the samples and slight compositional fluctuations that may occur from polymer to polymer. Above pH 7.5, the AMB COO^- groups are completely ionized, and the charge-balanced terpolymers exist as collapsed polyampholyte globules. The slight increases in viscosity above the solution IEPs for the polyampholytes are attributed to small charge excesses in the terpolymers; the uncompensated charges cause the collapsed polyampholytes globules to be stretched into elongated shapes.[11]

The AMDAP copolymers show similar, yet less profound, solution viscosity profiles as a function of pH. The PE peaks that occur at low pHs (due to protonation of the APDAP units) are shifted to lower pH values (by about 0.5 pH units) for the AMDAP copolymers because of the lower pK_a value of the APDAP COOH group. Although the AMBATAC terpolymers and AMDAP copolymers possess very similar cationic charge densities upon the complete protonation of the COO^- groups, the low-pH viscosities are much greater for the polyampholytes than for the polybetaines. The higher viscosities of the AMBATAC terpolymers at low pHs can be attributed to the chain-stiffening effects of the AMB functionality. Upon the ionization of the APDAP units with increasing pH, the polybetaine chains collapse due to intramolecular attractions between the zwitterionic groups, and this leads to a reduction in the solution viscosity. At the solution IEPs (pH $\approx$ 6), the AMDAP copolymers exhibit higher solution viscosities than the AMBATAC terpolymers; this observation indicates that the intramolecular attractions are stronger in the AMBATAC terpolymers. Indeed, the forces are much stronger in the AMBATAC terpolymers because the stiffer polyampholyte chains (i.e., due to the incorporation of AMB units) are able to collapse into smaller hydrodynamic volumes than the less rigid polybetaine chains. Above the solution IEPs, the AMDAP copolymers maintain relatively constant viscosities with increasing pH. No stretching of the collapsed AMDAP copolymers can be observed, as the polybetaines contain exactly equal numbers of cationic and
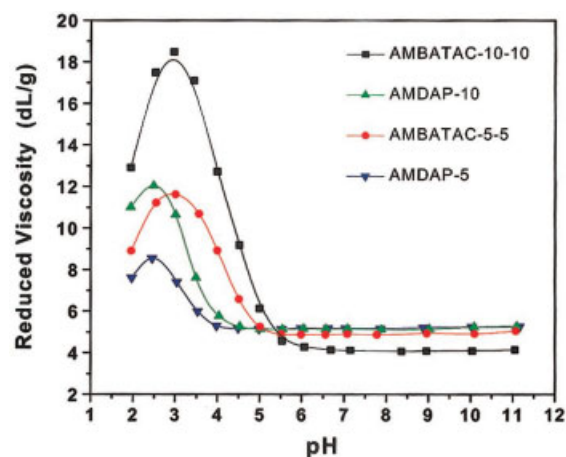
Figure 7 η_{red} of the AMBATAC terpolymers and AMDAP copolymers in $0.01M$ NaCl as a function of the solution pH ($c = 0.1$ g/dL).

anionic charges due to charge incorporation as a zwitterionic species.

At a low ionic strength

Figure 7 shows the dilute-solution ($c = 0.1$ g/dL) η_{red} values as a function of pH for the model PZs in $0.01M$ NaCl. Compared with the solution viscosities in DI water (Fig. 6), the η_{red} values at pH values of less than 5.0 are significantly lower in $0.01M$ NaCl because of the screening of the charge–charge repulsions between the cationic groups. The stretching of the AMBATAC terpolymers observed in DI water is eliminated by the addition of $0.01M$ NaCl (i.e., no viscosity increases are observed above the solution IEPs) because of the screening of the uncompensated charges by the added electrolyte. Above pH 5.5, the AMBATAC terpolymers exhibit lower solution viscosities than the AMDAP copolymers, and this indicates greater coil collapse in the polyampholytes due to stronger intramolecular forces.

At a high ionic strength

The pH-responsive η_{red} profiles of the model PZs in $0.5M$ NaCl are shown in Figure 8. In high-ionic-strength solutions, electrostatic interactions are virtually nonoperative because of extensive charge screening by the added electrolyte, leading to a pH response that is governed largely by hydrogen bonding and polymer chain stiffness rather than electrostatic factors. In the low-pH range (2–3), the PZs exist as cationic PEs that are collapsed because of the screening of electrostatic repulsions and intramolecular hydrogen-bonding associations between protonated COOH moieties. Hydrophobic effects due to the uncharged hydrocarbon portions of the ionic and zwitterionic
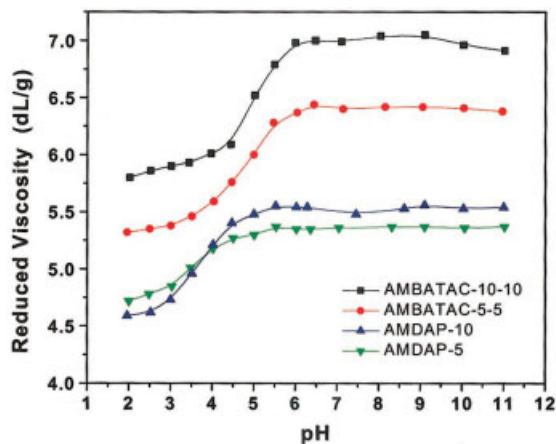
Figure 8 η_{red} of the AMBATAC terpolymers and AMDAP copolymers in 0.5M NaCl as a function of the solution pH (c = 0.1 g/dL).

comonomers may also contribute to this collapse. With increasing pH, the protonated COO^- groups of the AMB and APDAP units are neutralized, and the AMBATAC terpolymers and AMDAP copolymers exhibit PZ behavior. The magnitude of coil collapse with decreasing pH for the AMDAP copolymers increases as the zwitterionic comonomer content is doubled because of more intramolecular hydrogen-bonding associations with increasing APDAP incorporation. The AMBATAC terpolymers do not exhibit the same behavior with increasing comonomer content. Compared with AMBATAC-5-5, AMBATAC-10-10 exhibits a higher solution viscosity below pH 4, and this suggests that the positive excluded-volume contribution due to chain stiffness is greater than the negative excluded-volume contribution due to intramolecular hydrogen bonding between protonated AMB moieties.

Combined pH- and salt-responsive solution viscosity

To fully elucidate the pH- and salt-responsive behavior of the model PZs in dilute solutions, we measured the η_{red} values of AMBATAC terpolymer and AMDAP copolymer solutions (c = 0.1 g/dL) as a function of pH at several NaCl concentrations (Figs. 9 and 10). The three-dimensional (3D) plots shown in Figures 9 and 10 serve as phase diagrams that map the viscosity response to changes in the solution pH and salt concentration. The viscosity response is indicative of the solution behavior (i.e., PZ, PE, or combined PZ–PE) exhibited by the terpolymers at given values of the solution pH and NaCl concentration.

In Figure 9, four distinct regions can be observed in the plots for the AMBATAC-5-5 and AMBATAC-10-10 terpolymers:

1. At a low NaCl concentration and a low pH, a PE peak can be observed, corresponding to coil expansion due to unscreened electrostatic repulsions.
2. At a low NaCl concentration and a high pH, a polyampholyte valley can be observed, indicating coil collapse due to unscreened electrostatic attractions.
3. At a high NaCl concentration and a low pH, a PE valley can be observed, as the electrostatic repulsions are screened at higher ionic strengths and intramolecular hydrogen bonding predominates, leading to coil collapse.
4. At a high NaCl concentration and a high pH, a polyampholyte plateau can be observed, as the
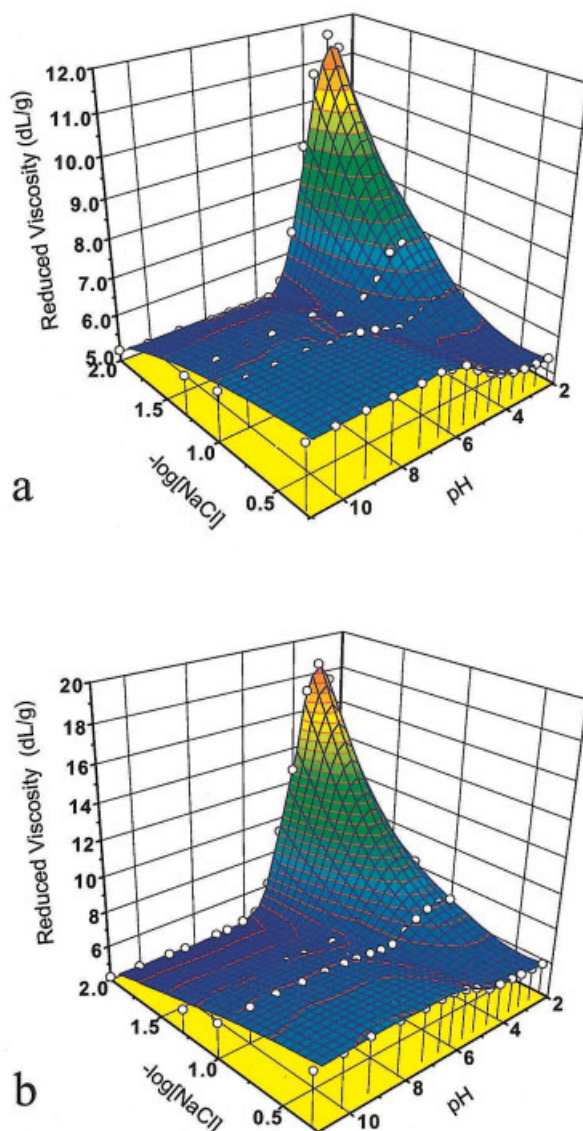
Figure 9 3D plots of η_{red} as a function of the NaCl concentration and solution pH for (a) AMBATAC-5-5 and (b) AMBATAC-10-10 (c = 0.1 g/dL). The open circles indicate actual data points.
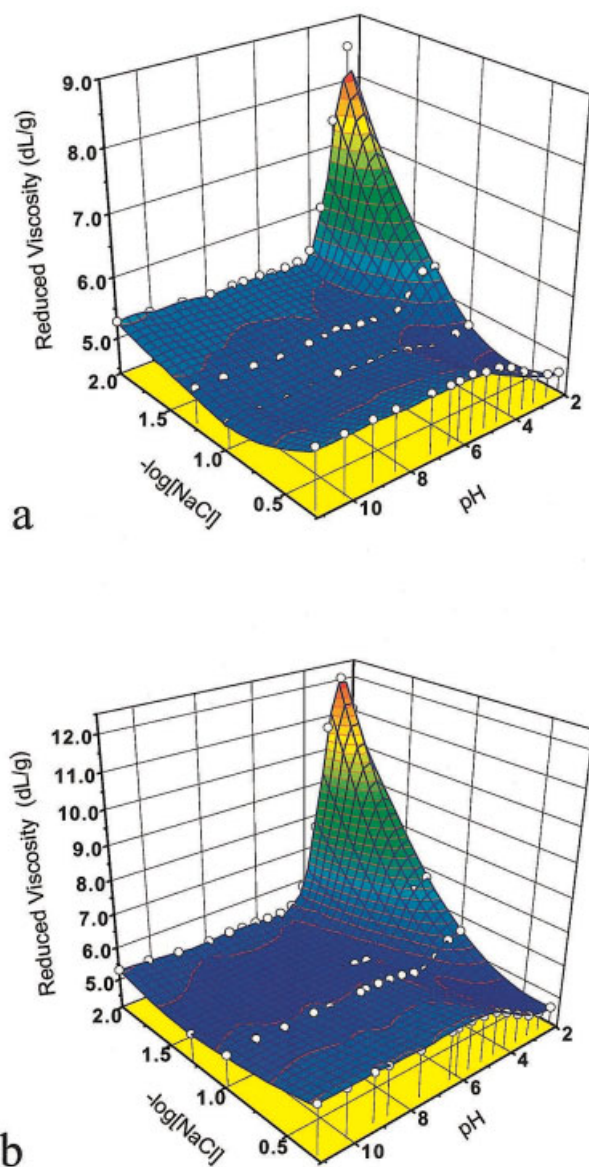
Figure 10 3D plots of η_{red} as a function of the NaCl concentration and solution pH for (a) AMDAP-5 and (b) AMDAP-10 (c = 0.1 g/dL). The open circles indicate actual data points.

increased ionic strength screens electrostatic attractions, allowing coil expansion.

Although the contours of the 3D plots for AMBATAC-5-5 and AMBATAC-10-10 are very similar, the magnitude of the solution viscosity response is significantly greater in AMBATAC-10-10 because of increased charge density.

The 3D plots for the AMDAP copolymers (Fig. 10) reveal less pronounced stimuli-responsive behavior in the polybetaines, as indicated by a flatter contour over much of the response space. Nonetheless, the AMDAP copolymers still exhibit the characteristic PE peaks at

low NaCl concentrations and low pHs and PE valleys at high NaCl concentrations and low pHs; however, the PZ response at high ionic strengths is relatively less in the polybetaines, and the AMBATAC terpolymers tend to maintain higher viscosities over wider ranges of the solution pH and NaCl concentration. For the AMDAP copolymers, the composite effect of weaker dipolar electrostatic interactions and decreased chain stiffness leads to less dramatic changes in the polymer conformation and hydrodynamic volume as functions of the solution pH and NaCl concentration and thus less distinct stimuli-responsive behavior of the polybetaine copolymers.

CONCLUSIONS

A series of model low-charge-density PZs, incorporating polyampholyte terpolymers composed of AM, NaAMB, and APTAC (AMBATAC) and polybetaine copolymers composed of AM and APDAP (AMDAP), were synthesized via conventional free-radical polymerization in aqueous media. The reaction conditions were selected to yield terpolymers with random charge distributions, homogeneous compositions, and well-defined MW and MWDs. Compositional analysis by ^{13}C-NMR revealed a good agreement between the monomer feed compositions and final polymer compositions. The model PZs were characterized extensively via SEC–MALLS analysis in a 0.1M NaCl phosphate buffer (pH 7) at 25°C. The SEC–MALLS analysis showed that the use of NaOOCH as a chain-transfer agent eliminates the effects of the monomer feed composition on DP, allows the control of the polymer MW, and suppresses excessively broad MWDs. The $[\eta]_{\text{SEC}}$ values determined with the Flory–Fox equation agree with the $[\eta]$ values determined via dilute-solution viscometry. An analysis of the R_g–M and MHS relationships for the model PZs provides information about the dependence of the macromolecular conformation and polymer–solvent interaction on the polymer structure and composition. SEC–MALLS and viscometric data indicate more open, random-coil conformations and greater polymer–solvent interactions in the AMDAP copolymers under SEC conditions. Potentiometric titration studies show that the AMBATAC terpolymers exhibit significantly higher apparent pK_a values than the AMDAP copolymers. The AMBATAC polyampholytes exhibit more pronounced stimuli-responsive solution viscosities and tend to maintain higher solution viscosities over wider ranges of the pH and NaCl concentration. The differences in the solution behavior observed for the AMBATAC polyampholytes and AMDAP polybetaines can be attributed to stronger electrostatic interactions and increased chain stiffness in the former.

References

1. Lowe, A. B.; McCormick, C. L. Chem Rev Press 2002, 102, 4177.
2. Kathmann, E. L.; McCormick, C. L. In Polymeric Materials Encyclopedia; Salamone, J. C., Ed.; CRC: Boca Raton, FL, 1996; Vol. 7, p 5462.
3. Salamone, J. C.; Rice, W. C. Encyclopedia of Polymer Science and Engineering, 2nd ed.; Mark, H. F.; Bikales, N. M.; Overberger, C. G.; Menges, G.; Kroschwitz, J. I., Eds.; Wiley-Interscience: New York, 1987; Vol. 11, p 514-530.
4. Candau, F.; Joanny, J. F. In Polymeric Materials Encyclopedia; Salamone, J. C., Ed.; CRC Press: Boca Raton, FL, 1996; Vol. 7, p 5476-5488.
5. Galin, J.-C. In Polymeric Materials Encyclopedia; Salamone, J. C., Ed.; CRC Press: Boca Raton, FL, 1996; Vol. 10, p 7189.
6. Kudaibergenov, S. E. Polyampholytes: Synthesis, Characterization, and Application; Plenum: New York, 2002.
7. Bekturov, E. A.; Kudaibergenov, S. E. Makromol Chem Macromol Symp 1989, 26, 281.
8. Bekturov, E. A.; Kudaibergenov, S. E.; Rafikov, S. R. J Macromol Sci Rev Macromol Chem Phys 1990, 30, 233.
9. Higgs, P. G.; Joanny, J. F. J Chem Phys 1991, 94, 1543.
10. Kantor, Y.; Li, H.; Kardar, M. Phys Rev Lett 1992, 69, 61.
11. Dobrynin, A. V.; Rubinstein, M. J Phys II 1995, 5, 677.
12. Kudaibergenov, S. E. Adv Polym Sci 1999, 144, 115.
13. Dobrynin, A. V.; Colby, R. H.; Rubinstein, M. Macromolecules 1995, 28, 1859.
14. Everaers, R.; Johner, A.; Joanny, J. F. Macromolecules 1997, 30, 8478.
15. Peiffer, D. G.; Lundberg, R. D.; Turner, S. R. U.S. Pat. 4,461,884 (1984).
16. Peiffer, D. G.; Lundberg, R. D.; Kowalik, R. M.; Turner, S. R. U.S. Pat. 4,460,758 (1984).
17. Peiffer, D. G.; Lundberg, R. D. Polymer 1985, 26, 1058.
18. Peiffer, D. G.; Lundberg, R. D. U.S. Pat. 4,710,555 (1987).
19. Schulz, D. N.; Peiffer, D. G.; Kowalik, R. M.; Kaladas, J. J. U.S. Pat. 4,560,710 (1985).
20. Schulz, D. N.; Kitano, K. U.S. Pat. 4,607,076 (1986).
21. Salamone, J. C.; Ahmed, I.; Rodriguez, E. L.; Quach, L.; Watterson, A. C. J Macromol Sci Chem 1988, 25, 811.
22. Watterson, A. C.; Liang, C. H.; Salamone, J. C. Polym Prepr 1990, 31, 497.
23. McCormick, C. L.; Johnson, C. B. J Macromol Sci Chem 1990, 27, 539.
24. McCormick, C. L.; Johnson, C. B. Polymer 1990, 31, 1100.
25. McCormick, C. L.; Salazar, L. C. Polymer 1992, 33, 4384.
26. McCormick, C. L.; Salazar, L. C. Polymer 1992, 33, 4617.
27. Watterson, A. C.; Liang, C. H.; Salamone, J. C. Polym Prepr 1992, 33, 276.
28. McCormick, C. L.; Salazar, L. C. J Appl Polym Sci 1993, 48, 1115.
29. Kathmann, E. E. L.; Davis, D. D.; McCormick, C. L. Macromolecules 1994, 27, 3156.
30. Neyret, S.; Candau, F.; Selb, J. Acta Polym 1996, 47, 323.
31. Ohlemacher, A.; Candau, F.; Munch, J. P.; Candau, S. J. J Polym Sci Part B: Polym Phys 1996, 34, 2747.
32. Kathmann, E. E.; McCormick, C. L. J Polym Sci Part A: Polym Chem 1997, 35, 231.
33. Kathmann, E. E.; McCormick, C. L. J Polym Sci Part A: Polym Chem 1997, 35, 243.
34. Kathmann, E. E.; White, L. A.; McCormick, C. L. Polymer 1997, 38, 871.
35. Kathmann, E. E.; White, L. A.; McCormick, C. L. Macromolecules 1997, 30, 5297.
36. Kathmann, E. E.; White, L. A.; McCormick, C. L. Polymer 1997, 38, 879.
37. Fevola, M. J.; Ezell, R. G.; Bridges, J. K.; McCormick, C. L. Polym Prepr 2003, 44, 1150.
38. Braun, O.; Selb, J.; Candau, F. Polymer 2001, 42, 8499.
39. McCormick, C. L.; Johnson, C. B. Macromolecules 1988, 21, 694.
40. McCormick, C. L.; Johnson, C. B. Macromolecules 1988, 21, 686.
41. McCormick, C. L.; Blackmon, K. P. J Polym Sci Part A: Polym Chem 1986, 24, 2635.
42. Liaw, D.-J.; Huang, C.-C.; Lee, W.-F.; Borbely, J.; Kang, E.-T. J Polym Sci Part A: Polym Chem 1997, 35, 3527.
43. The Merck Index, 11th ed.; Merck: Rahway, NJ, 1989; p 1362.
44. McCormick, C. L.; Blackmon, K. P.; Elliott, D. L. J Polym Sci Part A: Polym Chem 1986, 24, 2619.
45. McCormick, C. L.; Blackmon, K. P. U.S. Pat. 4,649,183 (1987).
46. McCormick, C. L.; Elliott, D. L. Macromolecules 1986, 19, 542.
47. McCormick, C. L.; Salazar, L. C. J Polym Sci Part A: Polym Chem 1993, 31, 1099.
48. McCormick, C. L.; Salazar, L. C. J Macromol Sci Chem 1992, 29, 193.
49. Salazar, L. C. Ph.D. Dissertation, University of Southern Mississippi, 1991.
50. Fevola, M. J.; Hester, R. D.; McCormick, C. L. J Polym Sci Part A: Polym Chem 2003, 41, 560.
51. Thomas, W. M.; Wang, D. W. In Encyclopedia of Polymer Science and Engineering, 2nd ed.; Mark, H. F.; Overberger, C. G.; Menges, G.; Kroschwitz, J. I., Eds.; Wiley-Interscience: New York, 1985; Vol. 1, p 176.
52. Gleason, E. H.; Miller, M. L.; Sheats, F. J Polym Sci 1959, 38, 133.
53. Fanood, M. H. R.; George, M. H. Polymer 1988, 29, 128.
54. Corpart, J. M.; Selb, J.; Candau, F. Polymer 1993, 34, 3873.
55. Laughlin, R. G. Langmuir 1991, 7, 842.
56. Schittenhelm, N.; Kulicke, W.-M. Macromol Chem Phys 2000, 201, 1976.
57. Yamakawa, H. Modern Theory of Polymer Solutions; Harper & Row: New York, 1971.
58. Tirrell, M. In Rheology: Principles, Measurements, and Applications; Macoscko, C. W., Ed.; VCH: New York, 1994; p 475.
59. Kurata, M.; Tsunashima, Y. In Polymer Handbook, 4th ed.; Grulke, E. A., Ed.; Wiley: New York, 1999; p 265.
60. Laughlin, R. G. Adv Liq Cryst 1978, 3, 41.
61. Laughlin, R. G. Adv Liq Cryst 1978, 3, 99.
62. Niu, A.; Liaw, D.-J.; Sang, H.-C.; Wu, C. Macromolecules 2000, 33, 3492.
63. McCormick, C. L.; Elliott, D. L.; Blackmon, K. P. Macromolecules 1986, 19, 1516.
64. McCormick, C. L.; Elliott, D. L. J Polym Sci Part A: Polym Chem 1987, 25, 1329.
65. McCormick, C. L.; Hutchinson, B. H.; Morgan, S. E. Makromol Chem 1987, 188, 357.
66. Munk, P.; Aminabhavi, T. M.; Williams, P.; Hoffman, D. E.; Chmelir, M. Macromolecules 1980, 13, 871.